ANL-HEP-CP-80-24

CONF-800374--11

ISSUES IN MASSIVE LEPTON PAIR PRODUCTION IN HADRONIC INTERACTIONS - 1980

by

Edmond L. Berger

Prepared for

Conference

XV Recontre de Moriond

Les Arcs, France

March 1980

ARGONNE NATIONAL LABORATORY, ARGONNE, ILLINOIS

Operated under Contract W-31-109-Eng-38 for the U. S. DEPARTMENT OF ENERGY

ANL-HEP-CP-80-24
April, 1980

ISSUES IN MASSIVE LEPTON PAIR PRODUCTION IN HADRONIC INTERACTIONS - 1980*

Edmond L. Berger
High Energy Physics Division
Argonne National Laboratory
Argonne, Illinois 60439

ABSTRACT

A discussion is presented of issues of current importance in the theory and phenomenology of massive lepton pair production in hadronic interactions. I emphasize the relevance of higher-twist inverse-power terms for all constituent scattering processes.

Invited review presented at the XV Rencontre de Moriond, Les Arcs, France, March, 1980.

*Work performed under the auspices of the United States Department of Energy.

I. INTRODUCTION

The basic approach for describing massive lepton pair production continues to be based on the parton model picture sketched in Fig.1. In this classical Drell-Yan model,[1,2] a quark of a given flavor from one of the initial hadrons is presumed to annihilate with an antiquark of the same flavor from the other hadron. The intermediate massive virtual photon decays into lepton pairs. The hadronic origins of the initial constituents are essentially ignored. The quark and the antiquark are assumed to be on-shell, massless, spin-½ constituents. Their momentum distributions are presumed to be identical to those measured in deep-inelastic lepton scattering. Predictions derived from this simple parton picture have been catalogued in many places.[2] I shall limit myself here to four of the salient of these (scaling, p_T spectra, absolute normalization, angular distributions) and shall compare them with excellent data presented earlier at this conference and elsewhere.[3,4,5] As discussed in Sec.II, the classical model has its shortcomings. Theorists have also been busy over the past few years. Within the context of quantum chromodynamics (QCD), various "higher-order" and "higher-twist" terms have been computed. These effects alter theoretical expectations significantly in some cases, and may explain the discrepancies between data and the classical Drell-Yan picture. In Secs.III and IV, I shall review some of the pertinent aspects and predictions of the higher-order and higher-twist amplitudes.

II. SOME EXPECTATIONS, SUCCESSES, AND FAILURES OF THE CLASSICAL MODEL

1. Scaling

According to the basic parton model, the cross-section for $hN \to \mu\bar{\mu}X$ should obey the simple scaling rule

$$\frac{M^4 d\sigma}{dM^2 dx_F} = f(M/\sqrt{s},\ x_F) \ , \tag{1a}$$

and the data behave as expected.[3-5] However, the prediction has really not been tested severely. For $0.2 \lesssim M/\sqrt{s} \lesssim 0.5$, Fermilab pN data[3] satisfy the expectation within 10 to 20% for $200 \le p_{lab} \le 400$ GeV/c and x_F near 0. Because deviations from exact scaling are perhaps only logarithmic in s at fixed $M/\sqrt{s}$ and x_F, it is necessary to compare data over a wider interval in s. Unfortunately, ISR data tend to be confined to values of $M/\sqrt{s} < 0.2$, eliminating the chance to make direct comparison with the FNAL results. The interval in $M/\sqrt{s}$ near $M/\sqrt{s} \simeq 0.2$ at $x_F = 0$ is also one for which scaling violations (i.e. explicit dependence on s at fixed $M/\sqrt{s}$ and x_F) are not expected to be large. Indeed, in deep-inelastic lepton scattering experiments,[6] the structure functions are observed to show little explicit Q^2 dependence near $x_{Bj} < 0.2$. Relatively large effects are observed at larger x_{Bj}, and for $x_{Bj} < 0.2$. Theoretically, scaling violations associated with either higher-twist or higher-order gluonic radiation effects should be most pronounced at large x_i. Thus, to observe significant departures

from scaling, it is necessary to obtain massive lepton pair data which extend into the large x_i region of the constituent structure functions ($M^2/s \simeq x_1 x_2$, $x_F = x_1 - x_2$).

2. p_T Spectra

In the classical model, the transverse momentum distribution of the massive lepton pair is provided by the ("primordial") transverse momentum fluctuations of the constituents in the initial hadrons. Therefore, $\langle p_T \rangle_{\mu\bar{\mu}}$ should be independent of incident energy s and "small". Here, "small" denotes a size typical of scaling hadronic processes, i.e. ~300 MeV. In contrast, the observed values of $\langle p_T^2 \rangle_{\mu\bar{\mu}}$ at fixed $M/\sqrt{s}$ grow with s, and the relationship

$$\langle p_T^2 \rangle_{\mu\bar{\mu}} = a \cdot s + b \qquad (2)$$

fits the facts.[2,3,4] Moreover, at energies typical of the SPS and Fermilab, $\langle p_T^2 \rangle_{\mu\bar{\mu}} \simeq 2$ GeV^2. The large energy dependent values of $\langle p_T \rangle_{\mu\bar{\mu}}$ are a clear indication that the classical model must be superceded. Higher-order gluonic radiation diagrams supply a qualitative interpretation of the behavior of the p_T spectra. However, there are significant quantitative problems for the QCD explanation, associated in part with the interplay of the gluonic radiative and higher-twist terms (including off-shell effects, and "primordial" k_T contributions). These issues as well as confrontations with data are discussed in my *ORBIS SCIENTIAE* review.[2]

3. Absolute Normalization

In the classical model, if the quark and anti-quark

structure functions have been determined from measurements of deep-inelastic lepton scattering, then the absolute normalization is predicted for $\sigma(pN \to \mu\bar{\mu}X)$. This prediction appears to fail by roughly a factor of $K \simeq 2$, with $\sigma_{exp} \gtrsim 2\sigma_{classical}$. As discussed by Decamp in his presentation at this meeting,[5] the discrepancy is true for π^-N, π^+N, pN, K^-N, and $\bar{p}N$ processes. I have certainly no vested interest in restoring the classical model, but I doubt that we have heard the final word on this issue of the K factor.

Experimentally, the factor of K is tied up with the A dependence of the cross-section. The highest statistics data are obtained from interactions on heavy nuclei such as Platinum with $A = 195$, and an extrapolation is made to the cross-section σ_0 per nucleon at $A = 1$. The NA3 group has a sample of data from π^-H_2 interactions, ~600 events with $M_{\mu\bar{\mu}} > 4.1$ GeV, which they compare with the π^-Pt sample of 21,600 events. They conclude that $\alpha \simeq 1.03 \mp 0.03$ if they fit to $\sigma = \sigma_0 A^{\alpha}$. I imagine that α is a function $\alpha(M, x_F)$, as is σ_0, but 600 events probably do not permit a detailed study of this variation. Although the value of α is determined only for π^-N collisions, the NA3 group uses the same value of α to extract σ_0 for their other processes as well. The NA3 value agrees with the determination of $\alpha = 1.02 \pm 0.02$ in pN processes by the Columbia-Fermilab-Stony Brook collaboration,[3] but disagrees with the value $\alpha = 1.12 \pm 0.05$ found by the Chicago-Illinois-Princeton group[4] (π^-N). If $\alpha \simeq 1.1$, then σ_0 is reduced by roughly the

required factor of 2.

The study of A dependence as a function of $M/\sqrt{s}$ and x_F is of interest in its own right and should be pursued. For the question of absolute normalization, it would be best to obtain a significant sample of events on hydrogen, especially in proton-antiproton processes. It is suggestive that in their study of the $\pi^- H_2$ data at 200 GeV/c, the NA3 group finds that there may be a strong M dependence of the K factor, with $K \simeq 2.4$ for $M \simeq 5$ GeV, but consistent with unity at $M \simeq 8$ GeV.

There is a different way to present the discrepancy in absolute rate. According to the classical model, the cross-section for $pN \to \mu\bar{\mu}X$ is proportional to a convolution of the quark and anti-quark distribution functions. If we take the relatively well determined quark distribution functions from deep-inelastic lepton processes, then the classical model formula and the $pN \to \mu\bar{\mu}X$ data can be used to measure the anti-quark content of the nucleon. This determination of the ocean can be compared with that from studies[6] of $\nu N \to \mu X$ and $\bar{\nu}N \to \bar{\mu}X$. The comparison is shown in Fig.2. We note that the neutrino data and the hadron data tend to probe the ocean in different intervals of x and $|Q^2|$. However, near $x \simeq 0.2$, where the $|Q^2|$ values also overlap, there is as much as a factor of two difference in absolute normalization.

Is the discrepancy due solely to the ocean? Probably not. Indeed, the NA3 group finds that the factor $K = 2.15 \mp 0.4$

for $\bar{p}N \to \mu\bar{\mu}X$ at 150 GeV/c. The $\bar{p}N$ process is dominated by valence-valence interactions. Unfortunately, the α dependence has not been measured directly for $\bar{p}N$ processes.

As I'll discuss in Sec.III, the factor $K \simeq 2$ may be a welcome development. Large next-to-leading order QCD radiative corrections have been calculated for the Dreil-Yan process. If it can be shown that these large terms do not invalidate the use of a perturbative expansion in QCD, then the K factor may be hailed eventually as a triumph.

4. Angular Distributions

Annihilation of on-shell spin-½ massless quarks and antiquarks in the Drell-Yan process leads to the unambiguous prediction that $d\sigma/d\cos\theta \propto (1 + \alpha\cos^2\theta)$ with $\alpha \equiv 1$.* Here θ is measured in the $\mu\bar{\mu}$ rest frame; it is the polar angle of the outgoing μ with respect to a $\hat{z}$ direction specified by the collinear q and $\bar{q}$ axis. Only hadron directions and not q (or $\bar{q}$) directions are measured, of course. Thus, some deviation from $\alpha = 1$ is expected, associated with the primordial k_T fluctuations of quarks and antiquarks in the initial hadrons. If the incident beam direction is chosen as the quantization axis, then a reduction to $\alpha \sim 0.8$ is a reasonable estimate[7] of the effects of primordial k_T. Experimentally, the expectation $d\sigma/d\cos\theta \propto (1 + \alpha\cos^2\theta)$ with $\alpha \simeq 0.8$ is well verified for data integrated over all x_F or over all p_T. However, for $\pi^-N \to \mu\bar{\mu}X$, both the Chicago-Illinois-Princeton[4] and the CERN NA3[5] groups have shown that α decreases system-

*It is regrettable that the same Greek letter α is used for A dependence and for angular distributions.

atically as x_F approaches 1 or as p_T grows. Thus, the classical expectation of $d\sigma/d\cos\theta \propto (1 + \cos^2\theta)$ is borne out only for small p_T and small x_F of the massive lepton pair. As either p_T or x_F grows, the data show that the massive virtual photon prefers to be polarized longitudinally. Data on the azimuthal angle variation would be welcome.

The data on angular distributions are thus a third piece of evidence against the classical model. Both higher-twist[8] and higher-order[9] QCD terms lead to deviations of α from unity. The higher-twist effects are important at large x_F whereas the higher order contributions grow in importance as p_T increases. I present a treatment of higher-twist effects in Sec.IV.

III. WHAT HAS QCD DONE FOR DRELL AND YAN?

As stated in the Introduction, the classical model[1] is equivalent to the premise that the only important amplitude is that in which an on-shell, spin-½, massless quark annihilates with a similarly on-shell, spin-½, massless antiquark, as in Fig.3(a) or Fig.4(a). Physics, as embodied in part in QCD, argues that other processes may also contribute significantly. These other processes are of two classes: higher-order and higher-twist.

1. Higher-order

Some of the higher-order processes[10] are sketched in Fig.3(b) - (h). The massive lepton pair (γ) may be produced through an interaction between a quark constituent from one hadron with a gluon constituent in the other. A few of these possibilities are shown in Fig.3(b), (c), (g), and (h). Likewise, the quark-antiquark interaction may result in the production of one or more gluons in addition to the massive lepton pair (e.g. Fig.3(d) and (e)). Massive virtual photons may be produced in a quark-quark collision of type $qq \to qq\gamma$; one such case is shown in Fig.3(f). This whole class is labeled "higher-order" for obvious reason. The term gluon radiative correction is also used frequently to include all the higher-order processes in which there is a gluon in the initial state, Figs.3(b), (c), (g), (h), or in which a gluon is emitted in the final state (e.g. Fig.3(d) and (e)). The examples sketched in Fig.3 are, of course, hardly exhaustive.

A great deal of study[10,11] has been devoted to diagrams such as sketched in Fig.3, not only for the Drell-Yan process but for other constituent scattering reactions including deep-inelastic lepton scattering, e^+e^- annihilation, and hadronproduction at large p_T. Indeed, gluonic radiative corrections provide logarithmic scaling violations in Q^2 about which we have heard so much in deep-inelastic scattering, and diagrams such as those sketched in Fig.3(b) and (c) supply the three jet events in the annihilation process $e^+e^- \to$ hadrons.

In the Drell-Yan process, the higher-order diagrams sketched in Fig.3 affect all theoretical expectations.[2] For example, the possibility of a gluon recoil such as shown in Fig.3(d) and (e) allows the massive virtual photon (γ) to be produced at large p_T, with $\langle p_T^2 \rangle \propto s$. In Figs.3(b) and (c), the quark recoil balances p_T. Second, just as in deep-inelastic lepton scattering, the gluonic radiation diagrams generate scaling violations. Thus, Eq.(1a) is replaced by

$$\frac{M^4 d\sigma}{dM^2 dx_F} = f\left(\frac{M}{\sqrt{s}}, x_F, s\right) . \tag{1b}$$

Third, the angular distribution in the lepton pair rest frame is changed.[9] As p_T grows at fixed x_F, the angular distribution $d\sigma/d\cos\theta$ is changed from $(1 + \alpha\cos^2\theta)$ with $\alpha \simeq 1$ to one in which $\alpha \simeq 0$. Finally, the overall normalization of the massive lepton pair cross-section may be altered significantly. This last issue is the subject of

considerable recent debate[11] and deserves a few comments.

After integration over transverse momentum, the cross-sections supplied by the various diagrams in Fig.3 may be expanded in a power series in $g^2 \ell n\, Q^2$, where $\alpha_s = g^2/4\pi$. Thus,

$$\begin{aligned}
\sigma_{(a)} &= q_0(x_1)\bar{q}_0(x_2)\left[1\right] \\
\sigma_{(b),(c)} &= q_0(x_1)G_0(x_2)\left[\alpha_s \ell n\, Q^2 + \alpha_s C_1^G\right] \\
\sigma_{(d),(e)} &= q_0(x_1)\bar{q}_0(x_2)\left[\alpha_s \ell n\, Q^2 + \alpha_s C_1^q\right] \\
\sigma_{(f),\ldots} &= q_0(x_1)q_0(x_2)\left[\alpha_s^2 \ell n^2 Q^2 + \alpha_s^2 \ell n\, Q^2 + \alpha_s^2 C_2\right]
\end{aligned} \tag{3}$$

Here, $q_0(x_i)$, $\bar{q}_0(x_i)$, and $G_0(x_i)$ are the quark, antiquark and gluon momentum distributions determined at some reference value of $Q_0^2 = M_0^2$; C_1 and C_2 are independent of $Q^2 = M_{\mu\bar{\mu}}^2$.

If we retain only the leading logarithmically divergent contributions in Eqs.(3) for each order in g^2 and sum to all orders, then the resulting sum collapses into a cross-section with the usual Drell-Yan form, but for one simple replacement: the quark and antiquark structure functions become explicit non-scaling functions of Q^2. Moreover, these new Q^2 dependent structure functions are identical to those measured at $|Q^2|$ in (spacelike) deep inelastic lepton scattering.

At the leading log level, therefore, QCD predicts that the absolute normalization of $h_1 N \to \mu\bar{\mu}X$ should be exactly that specified in terms of structure functions from deep-inelastic reactions, with $K = 1$, not the value $K \gtrsim 2$ observed experimentally (c.f. Sec.II). Surprises come at the next-to-leading-log level, however. In order g^2, the next-to-leading

log terms are those proportional to C_1^q and C_1^G in Eq.(3). Explicit calculations show that C_1^q is proportional to π^2 and is numerically large. Even though the next-to-leading log terms are reduced by $1/\ln Q^2$ (i.e. by α_s), their numerical strength is significant. Indeed, the leading and next-to-leading terms are roughly equal numerically for values of $M/\sqrt{s} \simeq 0.2$ where present data exist. This seems to be exactly what the data demand. However, theoretically, it is seriously troubling that the first and second terms in a perturbation series are of equal size. What of the third and fourth?

Present theoretical efforts[11] are directed towards proving that the large π^2 effect can be associated with a unique set of graphs (vertex corrections to $q\bar{q} \to \gamma$) which can, in turn, be summed to all orders in g^2 in a controlled way as in QED. If the dangerously large next-to-leading order contributions can <u>all</u> be included in the vertex correction set to all orders in g^2, in a gauge independent fashion, then this dangerous class can be summed separately and removed from the perturbation series. It may then be possible to demonstrate that the normalization discrepancy factor $K \gtrsim 2$ discussed in Sec.II is just what QCD ordered. To be sure, K will not turn out to be a constant. Theoretically, K should show significant dependence on $M/\sqrt{s}$ and x_F, and approach unity as $M^2 \to \infty$. To the extent that the large next-to-leading order corrections are all associated with summable vertex corrections of the $q\bar{q}$ variety, they should be equally important in all processes (e.g. pN as well as π^-N and $\bar{p}$N).

From this restricted point of view, there is no difference (or advantage) in dealing with valence-valence dominated reactions such as $\bar{p}N \to \gamma^* X$.

This whole business would obviously be more convincing if we theorists had put our act together earlier and predicted $K \gtrsim 2$ before the experimenters asked for it.

2. Higher-Twist

In all the diagrams sketched in Fig.3, the initial constituents are treated as isolated, free, essentially on-shell point-like systems. The hadronic origins of the initial constituents are ignored. The physical premise underlying this restricted class of diagrams is that the constituents act singly and that some impulse approximation argument justifies coupling the probe (γ) to one and only one constituent in each hadron, with no ("time" for) cross-talk (momentum routing) between the constituents in a given hadron.

Not all physical processes can be described as if the probe couples to only one isolated constituent. For example, in elastic scattering (e.g. $e\pi \to e\pi$ or $ep \to ep$) the quarks and other constituents in the π and p must all act coherently, sharing transverse momentum, and turning-the-corner-together. Likewise, in processes in which a particular exclusive channel is dominant, such as $\ell N \to \ell' N^*$, or $\ell N \to \ell' \Psi N$ the constituents of the nucleon must be reconfigured coherently into an N^* or the final N. Even in purely inclusive processes, such as $\ell N \to \ell' X$, coherence effects should play a role at some level, particularly at modest

values of Q^2 and/or for large values of x_{Bj}, where the exclusive and elastic channels are significant. If there is any important substructure in the nucleon ("diquarks"?), coherence effects could show up even at small x_{Bj}.

Higher-twist terms are associated with coherence phenomena. They address the physics of the hadronic origins of the initial constituents, taken two, three, ..., or more at one time. The term "higher-twist" has a clear meaning in the framework of the operator product expansion.[12] A higher-twist contribution arises whenever the probe (photon, $W^{\pm}$, Z ,...) can couple to more than the minimum number of elementary fermion fields. This idea is illustrated in Fig.4. In the scattering from hadrons, higher-twist effects are always present because a hadron is never just an isolated quark. At issue is the relative importance of the minimum twist and higher-twist terms. All the diagrams in Fig.3 are in the minimum twist 2 class.

Higher twist contributions to cross-sections are reduced by a power of Q^2 from the leading asymptotic scaling terms. They are inverse-power rather than logarithmic effects in Q^2. Obviously, their magnitude is set in part by some mass scale, transverse momentum scale, or other hadronic size effect. Thus, one expects to see non-scaling terms in cross-sections proportional to m^2/Q^2, to Λ^2/Q^2, or to k_T^2/Q^2, and powers thereof. Here, m denotes a quark mass or a hadron mass. Second, higher-twist terms may have a dependence on kinematic variables such as x, z, and $M/\sqrt{s}$ different from

that of the asymptotically dominant minimum twist terms. In cases in which they have been computed, the higher twist terms decrease less rapidly with $(1-x)$ as $x \to 1$, by one or two integer powers.[8,13,14] They also have different spin properties from the minimum twist terms.[8] Regardless of how high one rises in Q^2, the effects of the higher-twist terms are dominant for values of x or z close enough to unity. When results are reexpressed in terms of moments over x, the different x dependences of minimum and higher-twist terms are reflected in N dependence, with higher-twist effects growing with N as N/Q^2, as N/Q^4, or as $N(N-1)/Q^2$, relative to the minimum twist term.

A complete calculation has yet to be made leading to a firm estimate for the magnitude and expected form of higher-twist effects in deep-inelastic scattering from a nucleon target.[13] Results for scattering from a "pion" target are described in Sec.IV. They are relevant for the experimentally measurable reactions $\pi N \to \mu\bar{\mu}X$ and $\ell N \to \ell'\pi X$.

Higher-twist effects may be regarded as a nuisance if one's preference is to concentrate on the non-scaling $\ell n\, Q^2$ effects associated with gluonic radiative corrections. Unless excellent data are available over a range in Q^2 extending to very high values, it is obviously possible to fit results equally well with inverse power terms $(1/Q^2)^n$ or with $1/\ell n\, Q^2$ effects. Logarithmic scaling violations have long been advertised as a crucial test of QCD.[15] However, at high Q^2, $\ell n\, Q^2$ deviations from perfect scaling become vanishingly small. At low Q^2, the $1/Q^2$ and $1/Q^4$

terms become important. Abbott and Barnett have shown that the interpretation of the observed Q^2 dependence in deep-inelastic data is ambiguous.[16]

Higher-twist terms appear also to play an important role in large p_T hadron physics. For example, the standard minimum twist QCD approach[17] must be supplemented by rather large contributions from "primordial" k_T smearing. The convolution modifies the magnitude and shape of the large-p_T cross-section significantly even at $p_T \sim 6$ GeV/c. The large dose of primordial k_T needed to describe hadron production and massive lepton pair production at large p_T implies that the initial constituents are significantly off-shell:[18] $p^2 \simeq k_T^2/(1-x)$. Thus, coherence effects and hadronic bound state properties must be treated properly. The same type of pionic bound state effects which lead to the significant $\sin^2\theta$ effect in the angular distribution for $\pi^- N \to \mu\bar{\mu}X$ at large x_F will also lead to a large p_T^{-6} component in the cross section for $hh \to \pi X$ at large p_T.[14] Finally, in the study of three-jet and other phenomena in e^+e^- annihilation processes, the detailed interplay of basic QCD results and ad-hoc fragmentation functions is critical for obtaining precise fits to data. The fragmentation effects necessarily involve coherence and, thus, higher-twist physics is implicated again.

The need is clear for precise phenomenological estimates of the magnitude and kinematic dependence of higher-twist effects in all inclusive and semi-inclusive constituent

scattering processes. We should give the experimenters some predictions to shoot at! One faces both perturbative and non-perturbative issues. Because QCD has not yet been shown to provide the spectrum of hadrons observed in Nature, or, indeed, any bound states of constituents, coherence phenomena cannot be calculated in detail with this theory. In particular, the non-perturbative single-quark and single-gluon momentum distributions $q_0(x,Q_0^2)$ and $G_0(x,Q_0^2)$ are not really calculable in a model-independent way; only their evolution with Q^2 is predicted in perturbative QCD. Analogously, there will be some non-perturbative functions describing the higher-twist joint momentum distributions for several constituents in a hadron. The Q^2 evolution of these joint probabilities is presumably calculable perturbatively. These joint momentum distributions should be universal process-independent functions, as are the $q(x,Q^2)$ and $G(x,Q^2)$. Once extracted from the data for one reaction they can be used elsewhere. To obtain the explicit higher-twist contribution to the cross-section for a given process, an explicit perturbative point cross-section would be convoluted with the joint momentum distributions.

The emergence of higher-twist effects introduces inevitable new levels of complexity and ambiguity in the interpretation of data. Any simple conclusions drawn in the past from QCD fits must be reevaluated. Higher-twist and higher-order QCD effects must both be considered. At relatively low values of Q^2, higher-twist effects are very likely more important than higher-order phenomena. As an example, non-

factorization in x and z of the semi-inclusive cross-section $\ell N \to \ell' hX$ is a natural consequence of higher-twist physics.[14,19] Fortunately, there are indications from explicit calculations that higher-order and higher-twist terms yield different, distinguishable measureable effects in different parts of phase space. Spin effects such as σ_L may be a good high-twist filter.[8,13,19] Because higher-twist terms represent coherence and quark binding phenomena, important physics will be elucidated once we have been able to isolate and study their effects in the data.

In the next section I describe a specific calculation[8] of higher twist effects in $\pi^- N \to \mu\bar{\mu}X$. This calculation involves a model for the pion and thus includes an explicit evaluation of the large x behavior of the minimum-twist single quark momentum distribution function $q_\pi(x) \propto (1-x)^2$, and the higher-twist joint momentum distribution is shown to behave as $(1-x)^0/Q^2$.

IV. $\pi^- N \to \mu\bar{\mu} X$

I shall discuss the process

$$\pi^- N \to \mu\bar{\mu} X, \text{ at large } Q^2 = M^2_{\mu\bar{\mu}} , \tag{4a}$$

as a specific example of higher-twist terms.[8] As will be seen, the higher-twist piece does not come from a separate diagram which has to be "added". The full amplitude I derive includes both the basic minimum twist term (the usual Drell-Yan expression) and a higher-twist piece, with specified relative normalization. In the lowest order QCD perturbative Feynman diagram for $\pi^- N \to \mu\bar{\mu} X$, the pion appears explicitly as a $q\bar{q}$ system in a definite spin state. If I were to ignore bound state effects, and treat the quarks and antiquarks in the pion as free, then I would obtain the usual classical Drell-Yan prediction. However, by including bound-state effects, I obtain a cross-section which includes the classical term as well as an additional higher-twist term associated with the bound state. The cross-section and polarization state of the $(\mu\bar{\mu})$ system are predicted to depend in a detailed way on the internal dynamics of the pion. Analogous results[19] are true for

$$\ell N \to \ell' \pi X, \text{ at large } Q^2 = (p_\ell - p'_\ell)^2 . \tag{4b}$$

In the parton model and in the conventional QCD approach to processes such as those in Eqs.(4), it is customary first to isolate a basic pointlike constituent scattering process. The overall cross section is then expressed as a product of three incoherent probabilistic factors, representing (i) the

density of "free" on-shell constituents of the hadrons in the initial state, (ii) the constituent to constituent scattering cross section, and (iii) the probability that the "free" on-shell final constituent "decays" into the observed final state hadrons. The work described here is motivated by a desire to go beyond this simple approach, and to deal with the fact that constituents are not free, but are always bound in hadronic wave functions and are often considerably off-shell.[18] Indeed, at large x and/or at large z, constituents are pulled far off-shell. Accordingly, bound state effects not normally considered should grow in relevance, and the standard quark-parton model assumption of on-shell constituents becomes increasingly questionable. One of the consequences of on-shell behavior is the dominance of the cross sections associated with transversely polarized virtual photons and W's. When spin-½ constituents are far off-shell, however, the longitudinally polarized cross sections may take over, resulting in substantial changes in e.g., observable angular distributions. Data should be examined in an effort to establish this qualitative effect, regardless of the details of the specific model for bound state, off-shell behavior presented here.

The pion is a relativistic many-body system and no pretense is made here that is being described completely. However, in some well defined regions of phase space, in which the active quark (or anti-quark) constituent is far off-shell, the relevant large momentum behavior of the wave function

can be handled with first order QCD perturbation theory, i.e., by single gluon exchange.[20] The specific region of phase space amenable to this treatment is that in which the fractional longitudinal momentum x of the constituent is large, $x \gtrsim 0.5$.

Consider the process sketched in Fig.5(a) in which a quark constituent is removed from the pion. If this quark carries longitudinal momentum fraction x [light-cone variable] and transverse momentum k_T, relative to the initial pion's direction, then energy momentum conservation may be used to show that

$$p_a^2 = - \frac{k_T^2 + xM_X^2}{(1-x)} + xm_\pi^2 \ . \qquad (5)$$

Here M_X is the mass of the on-shell spectator recoil system, and p_a^2 is the square of the four-vector momentum of the active quark. Equation (5) indicates that if x is large and/or k_T^2 is large, the quark is far off-shell (and spacelike). This large momentum (p_a^2 large) behavior of the pion wave function may then be approximated by single gluon exchange, as sketched in Fig.5(b). In the specific calculations discussed below, I treat the on-shell spectator system, the upper line in Fig.5(b) as a single on-shell massless quark. Calculations can be done in which the spectator system is taken instead to be a state of several quarks and gluons. However, such diagrams yield contributions to cross sections which decrease with a greater power of $(1-x)$ [or of $(1-z)$] than for the leading terms which I retain.

I now discuss the reaction[8] $\pi^- N \to \mu\bar{\mu} X$. The dominant contribution to $\pi^- N \to \mu\bar{\mu} X$ at large $Q^2 = (p_\mu + p_{\bar{\mu}})^2$ arises from the annihilation $\bar{u}u \to \gamma^* \to \mu\bar{\mu}$, where the antiquark $\bar{u}$ comes from the π^- and u from the nucleon. It is conventional to treat both the incident u and the incident $\bar{u}$ as free, on-shell, massless constituents. Doing so, one obtains immediately the prediction that the angular distribution of the final lepton should follow the form $d\sigma/d\cos\vartheta \propto (1 + \alpha\cos^2\vartheta)$, with $\alpha = 1$. This form is characteristic of the coupling of a transversely polarized virtual γ^* to on-shell fermions. Here $\cos\vartheta = \hat{p}_\mu \cdot \hat{p}_{\bar{\mu}}$ is defined in the $\mu\bar{\mu}$ rest frame.

As the longitudinal momentum fraction x_F of the $\mu\bar{\mu}$ pair is increased towards its kinematic limit, or as $\tau = Q^2/s \to 1$ at fixed x_F, the annihilating antiquark in the pion is forced to carry a large fractional momentum x and is pulled off-shell. Accordingly, bound state and longitudinal polarization effects grow in potential importance. I concentrate on the kinematic region where only the $\bar{u}$ is far off-shell (i.e., $x_F \to 1$). It is sufficient to treat the u quark as nearly free and on-shell. Thus, the incident nucleon structure is ignored, and I specialize to the reaction $\pi^- q \to \gamma^* q$.

Relying on the discussion above, one may draw the two lowest-order diagrams shown in Fig.6. Both diagrams in Fig.6 are required by gauge invariance. The incident meson momentum p is partioned equally between the constituent d and $\bar{u}$. If this simplifying approximation is discarded,

a modest change occurs in the prediction of the relative size of the transversely polarized and longitudinally polarized components of the final cross section.

The invariant amplitude corresponding to Fig.6 is

$$\mathcal{M} \propto \bar{u}(p_+)\,\gamma_\mu\, v(p_-)\,\frac{1}{Q^2}\,\frac{\alpha_s(k^2)}{k^2}\,\Psi_\pi(\vec{0})$$

$$\sum_\lambda \bar{u}(p_1)\,\gamma_\alpha\, u_\lambda(p/2)\;\bar{v}_{-\lambda}(p/2) \tag{6}$$

$$\left[-\gamma^\alpha\,\frac{i}{\not{p}_a + m}\,\gamma^\beta + \gamma^\beta\,\frac{1}{\not{p}_c - m}\,\gamma^\alpha\right] u(p_b)\ .$$

Here m denotes the quark mass. The equality $\sum u_\lambda \bar{v}_{-\lambda} = (\tfrac{1}{2}\not{p} + m)\gamma_5$ specifies that the $\bar{u}d$ bound state is a pseudoscalar. The factor $\Psi_\pi(\vec{r} = \vec{0})$ in Eq.(6) represents an integration over the unspecified soft momenta in the pion wave function. Note that in this calculation the quark transverse momentum k_T enters explicitly.

For simplicitly in what follows, I set $m^2 = 0$ and $m_c^2 = 0$, and restrict attention to $k_{Ta}^2 \ll Q^2$. Using the amplitude in Eq.(6), one may compute an explicit expression for the cross section for $\pi^- N \to \mu^+\mu^- X$.

$$\frac{Q^2\,d\sigma}{dQ^2 d^2\vec{Q}_T dx_L d\cos\theta\, d\phi} = \int d^2\vec{k}_{Ta}\,dx_a\,d^2\vec{k}_{Tb}\,dx_b\,G_{q/N}(x_b, \vec{k}_{Tb})$$

$$\cdot\,\frac{\Psi_\pi^2(\vec{0})}{k_{Ta}^4}\left[(1-x_a)^2(1+\cos^2\theta) + \frac{2}{3}\sqrt{\frac{4k_{Ta}^2}{Q^2}}\,(1-x_a)\cos\theta\sin\theta\cos\phi\right. \tag{7}$$

$$\left. + \frac{4}{9}\,\frac{k_{Ta}^2}{Q^2}\sin^2\theta\right]\delta^{(2)}(\vec{Q}_T - \vec{k}_{Ta} - \vec{k}_{Tb})\,\delta(x_L - x_a - x_b)\,\delta(Q^2 - x_a x_b s)\ .$$

The angles θ and ϕ are defined in the $\mu\bar{\mu}$ rest frame. In this frame, the polar ($\hat{z}$) axis is chosen along the direction of the incident pion; $\cos\theta = \hat{p}_\mu \cdot \hat{p}_\pi$. The ($\hat{x},\hat{z}$) reaction plane is the plane defined by $\vec{p}_X$ and $\vec{p}_\pi$, with $\vec{p}_X$ chosen to have a positive component of momentum along $\hat{x}$. The azimuthal angle ϕ is measured with respect to $\hat{x}$. In the approximation in which I am working, $\vec{p}_X = \vec{p}_1$. In practice, some smearing of the angular distribution predicted in Eq.(7) is to be expected from the non-zero nucleon constituent transverse momentum $\vec{k}_{Tb}$ which I have neglected. In Eq.(7), $\vec{Q}_T$ is the transverse momentum of the lepton pair, and $G_{q/N}$ is the quark structure function of the nucleon.

To obtain Eq.(7), an expansion in inverse powers of Q^2 was performed, and discarded from the square brackets were subasymptotic terms which are of order $Q^{-2}k_{Ta}^2(1-x_a)$ and $Q^{-4}k_{Ta}^4(1-x_a)^{-1}$. The contributions from sea quarks and anti-quarks in the meson and nucleon are also ignored in Eq.(7). Equation (7) is accurate in two $Q^2 \to \infty$ limits: (a) the fixed x_a Bjorken limit, and (b) the fixed $W^2 = (1-x_a)Q^2/x_a$ limit, with $W^2 >> k_{Ta}^2$. The neglected terms in Eq.(7) must be retained at modest Q^2 for x_a very close to $1 (> 0.95)$. If scalar instead of vector gluons were used in the amplitude, the only changes in Eq.(7) would be the replacement of the factor (4/9) by the factor 4, and (2/3) by 2. As Eq.(7) stands, it would appear that the cross section diverges as $\vec{k}_{Ta} \to 0$. However, a finite answer should be obtained once finite masses are restored and the full confining properties implied by $\psi(\vec{0})$

are implemented explicitly.

In the Bjorken scaling limit, $Q^2 \to \infty$, at fixed x_a, the valence quark structure function of the pion can be extracted from Eq.(7):

$$G_{\bar{q}/\pi}(x) = \int d^2\vec{k}_T G_{\bar{q}/\pi}(x,\vec{k}_T) \propto (1-x)^2 \ . \tag{8}$$

The corresponding k_T fall-off produces pairs with a Q_T^{-4} distribution (for $k_{Ta}^2 << Q^2$).

We observe the following additional features of Eq.(7):

(i) We can identify a non-scaling contribution to the structure function. After averaging over $\cos\theta$ and over ϕ, we obtain:

$$G_{\bar{q}/\pi} \to (1-x)^2 + \frac{2}{9}\frac{\langle k_{Ta}^2\rangle}{Q^2} \ . \tag{9}$$

The non-scaling contribution is independent of x and will dominate the scaling contribution at fixed $Q^2(1-x)$ as $Q^2 \to \infty$. In this model the relative magnitude of the scaling and non-scaling terms is fixed.

(ii) The non-scaling $1/Q^2$ contribution corresponds to a <u>longitudinal</u> structure function and provides a $\sin^2\theta$ term in the angular distribution $d\sigma/d\cos\theta$, in contrast to the conventional expectation of $(1+\cos^2\theta)$. At fixed Q^2, the $\sin^2\theta$ term dominates in the cross section as $x_F \to 1$. The usual rule that annihilating spin-½ quarks produce transversely polarized photons is modified when off-shell constituents are involved. Here the $\bar{q}$ is kinematically far off-shell

since, as $x_F \to 1$, all of the momentum of the recoil spectator quark must be transferred to the annihilation subprocess. In this situation the spin of the incident meson influences the final angular distribution. The bound state effect is a high-twist subprocess, since more than the minimum number of elementary fields is required. Although the large x_F limit is stressed here, the $\sin^2\theta$ term should be important also at fixed x_F when $\iota = Q^2/s \to 1$. In this latter limit, $x_a \to 1$ also.

(iii) A significant non-scaling, non-isotropic azimuthal angle dependence $d\sigma/d\phi$ is predicted in Eq.(7). At fixed Q^2, the coefficient of the $\cos\phi$ term in the square brackets of Eq.(7) grows as $(1-x_a)^{-1}$ relative to the dominant scaling term. In general, one may also expect contributions to $d\sigma/d\phi$ proportional to $\cos 2\phi \sin^2\theta$. However, in this model, the $\cos 2\phi$ terms enter multiplied by factors such as $Q^{-2}k_{Ta}^2(1-x_a)$ and are therefore discarded in the approximation to which I am working.

Subsequent to these predictions, the change of the angular distribution $d\sigma/d\cos\theta$ with x, predicted in Eq.(7), was observed by the Chicago-Illinois-Princeton (CIP) collaboration.[4] The effect has now been confirmed at the CERN-SPS by the NA3 Collaboration.[5] The CIP results are shown in Fig.7. These results should encourage a much more detailed experimental investigation of the large x_F region in $\pi^- N \to \mu\mu X$, with broad angular coverage so that the distribution $d\sigma/d\cos\theta\, d\phi$ can be obtained precisely.

In Eq.(7), the strength of the $\sin^2\theta$ term grows linearly with k_{Ta}^2. Consequently, for any x_a, the $\sin^2\theta$ effect should be more pronounced at large $|\vec{Q}_T|$. Such an effect is indeed observed by the NA3 group[5] when they divide their data sample into subsets with $|\vec{Q}_T| < 1$ GeV/c and $|\vec{Q}_T| > 1$ GeV/c. The importance of QCD gluonic radiative diagrams (Fig.3) should also increase as $|\vec{Q}_T|$ grows. These terms contribute additional sources of $\sin^2\theta$ effects,[9] but are not responsible for a change of α with x at fixed $|\vec{Q}_T|$. Likewise, deviations of α from 1 may result from primordial k_T fluctuations,[7] but these deviations also do not vary with x_F. A complete calculation of the angular distribution is in progress in which both higher-twist and higher-order QCD effects are included.

In baryon (or antibaryon) induced reactions, $BB \to \mu\bar{\mu}X$, the $1 + \cos^2\theta$ behavior characteristic of spin-½ systems is maintained as $x \to 1$, in spite of the fact that an annihilating constituent is again far off-shell. It would be very valuable to verify this expectation experimentally. Non-scaling longitudinal contributions should arise near $x = 2/3$ if we take into account the subprocess $(qq) + \bar{q} \to q + \gamma^*$ with an integer-spin diquark system.[13] These effects may be related to the anomalous value of σ_L/σ_T observed in deep inelastic electron scattering at moderate values of Q^2.

The dominance of the longitudinally polarized cross section ($\propto \sin^2\theta$) as $x_F \to 1$ in $\pi N \to \gamma^* X$ is a direct indication that in this limit the annihilating antiquark carries the signature

of its origins in a spin zero meson. Observation of the $\sin^2\theta/Q^2$ term in the data is the first direct identification of a higher-twist effect in an inclusive reaction. The importance of this higher-twist effect in $\pi^- N \to \mu\bar{\mu}X$, for values of Q^2 as large as ~20 GeV^2, indicates that higher-twist effects should be examined carefully in all other high energy processes as well.[14,19]

V. CONCLUSIONS

Substantial progress is being made in calculations of both higher twist and higher order terms in QCD perturbation theory. There is good evidence in massive lepton pair data for one higher twist effect, in the angular distribution $d\sigma/d\cos\theta$. Higher order effects are suggested by the behavior of the p_T distribution $d\sigma/dp_T^2$ and by the discrepancy in absolute normalization of $d\sigma/dM^2dx_F$ (the "K factor"). Much solid work remains to be done by phenomenologists leading to estimates of the expected magnitude and kinematic dependence of higher-twist contributions in all inclusive and semi-inclusive constituent scattering processes.

REFERENCES

1. S. D. Drell and T. M. Yan, Phys. Rev. Lett. 25, 316 (1970), 25, 902 (1970), and Ann. Phys. (N.Y.) 66, 578 (1971). For a recent general discussion, see C. S. Lam and Wu-Ki Tung, Phys. Rev. D18, 2447 (1978).

2. E. L. Berger, ORBIS SCIENTIAE, 1979, Coral Gables, Florida, and SLAC-PUB-2314 (April, 1979), and references therein.

3. Columbia-Fermilab-Stony Brook Collaboration, J. K. Yoh et al., Phys. Rev. Lett. 41, 684 (1978) and 41, 1083 (1978), plus references cited therein; L. Lederman, Proceedings of the 19th International Conference on High Energy Physics, Tokyo, 1978. Edited by S. Homma, M. Kawaguchi and H. Miyazawa.

4. Chicago-Illinois-Princeton Collaboration, C. B. Newman et al., Phys. Rev. Lett. 42, 951 (1979); G. E. Hogan et al., Phys. Rev. Lett. 42, 948 (1979); K. J. Anderson et al., Phys. Rev. Lett. 42, 944 (1979) and Phys. Rev. Lett. 43, 1219 (1979).

5. CERN NA3 Experiment. CERN-College de France-Ecole Polytechnique-Orsay-Saclay Collaboration. Results presented at this conference by D. Decamp.

6. CERN-Dortmund-Heidelberg-Saclay Collaboration, J. G. H. deGroot et al., Zeitschrift fur Physik C1, 143 (1979); Aachen-Bonn-CERN-London-Oxford-Saclay Collaboration, P. C. Bosetti et al., Nucl. Phys. B149, 13 (1979) and B142, 1 (1978); Harvard-Chicago-Illinois-Oxford Collaboration, W. A. Loomis et al., Fermilab Report 78/94-Exp.

(1978), and H. L. Anderson et al., Phys. Rev. Lett. 40, 1061 (1978).

7. E. L. Berger, J. Donohue and S. Wolfram, Phys. Rev. D17, 858 (1978); J. Donohue in Phenomenology of Quantum Chromodynamics, Recontre de Moriond, 1978, ed. by J. Tran Thanh Van, Vol. 1, p. 159; E. L. Berger in New Results in High Energy Physics - 1978, Vanderbilt Conference, ed. by R. S. Panvini and S. E. Csorna, p. 178; J. C. Collins and D. E. Soper, Phys. Rev. D16, 2219 (1977).
8. E. L. Berger and S. J. Brodsky, Phys. Rev. Lett. 42, 940 (1979).
9. K. Kajantie, J. Lindfors and R. Raitio, Phys. Lett. 74B, 384 (1978); J. Cleymans and M. Kuroda, Phys. Lett. 80B, 385 (1979); J. C. Collins, Phys. Rev. Lett. 42, 291 (1979).
10. For an excellent review of higher order calculations, see A. J. Buras, Fermilab Report PUB-79/17-THY, published in Rev. Mod. Phys. 52, 199 (1980).
11. See, for example, G. Parisi, Phys. Letters 90B, 295 (1980); G. Altarelli, R. K. Ellis, and G. Martinelli, Nucl. Phys. B143, 521 (1978) plus Erratum B146, 544 (1978), and MIT preprint CTP 776 (1979); G. T. Bodwin, C. Y. Lo, J. D. Stack and J. D. Sullivan, Illinois report ILL-TH-80-02 (Jan. 1980); and G. Martinelli, presentation at this Moriond meeting.
12. D. J. Gross and S. B. Treiman, Phys. Rev. D4, 1059 (1971); S. Gottlieb, Nucl. Phys. B139, 125 (1978).
13. For estimates based on the idea of diquark substructure, see I. Schmidt and R. Blankenbecler, Phys. Rev. D16, 1318 (1977);

I. Schmidt, SLAC Report-203, Ph.D. Thesis submitted to Stanford University (1977); A. Fernandez-Pacheco, J. A. Grifols and I. A. Schmidt, Lett. Nuovo Cimento 22, 339 (1978); L. F. Abbott, E. L. Berger, R. Blankenbecler and G. L. Kane, Phys. Letters B88, 157 (1979), and references therein.

14. E. L. Berger, Zeitschrift für Physik C, to be published; SLAC report SLAC-Pub-2362 (July, 1979).

15. H. Georgi and H. D. Politzer, Phys. Rev. D9, 416 (1979).

16. L. F. Abbott and R. M. Barnett, SLAC-Pub-2325 (May, 1979), and L. F. Abbott, W. B. Atwood, and R. M. Barnett SLAC-Pub-2400 (Sept. 1979).

17. R. P. Feynman, R. D. Field and G. C. Fox, Nucl. Phys. B128, 1 (1977).

18. R. R. Horgan and P. N. Sharbach, Phys. Letters 81B, 215 (1979); W. E. Caswell, R. R. Horgan and S. J. Brodsky, Phys. Rev. D18, 2415 (1978).

19. E. L. Berger, Phys. Letters B89, 241 (1980).

20. For a detailed discussion, see S. J. Brodsky and G. P. Lepage, SLAC-Pub-2447, presented at the Summer Institute on Particle Physics, SLAC, 1979.

FIGURE CAPTIONS

1. Basic Drell-Yan quark-antiquark annihilation mechanism for lepton pair production in hadronic collisions, illustrated here for $h_a h_b \to \mu\bar{\mu}X$; $\bar{q}$ and q denote respectively an antiquark and a quark constituent.
2. A comparison of the sea distribution obtained from $pN \to \mu\bar{\mu}X$ via the classical Drell-Yan formula with that determined in deep-inelastic neutrino scattering. This figure is taken from Ref.2. The pN data are from Ref.3 and the neutrino points are extracted from the CDHS data of Ref.6 by a procedure described in Ref.2.
3. Series of diagrams illustrating the interactions of free quark, antiquark, and gluon constituents: (a) the basic zero order Drell-Yan process $q\bar{q} \to \gamma^*$; (b) and (c) the first order $O(\alpha_s)$ Compton processes $qG \to \gamma^* q$; (d) and (e) the first order two body annihilation process $q\bar{q} \to \gamma^* G$; (f), (g) and (h), a sample of second order, $O(\alpha_s^2)$, processes. Not drawn are many other diagrams in $O(\alpha_s^2)$ related by gauge invariance requirements to those shown.
4. (a) The basic *minimum-twist* 2 $q\bar{q} \to \gamma^*$ diagram.
   (b) A higher twist diagram.
5. (a) Vertex in which a quark is removed from an incident π; $\pi \to qX$. The quark carries four-momentum p_a.
   (b) The shaded oval represents the full wave function for pion dissociation into an on-shell system (upper line marked with an on-shell cross x) and an off-shell quark p_a carrying four-momentum squared p_a^2. In the

large p_a^2 limit, the large momentum behavior of the full wave function can be represented by single gluon exchange, as sketched on the right-hand side of (b). The unshaded oval stands for the pion wave function at small momentum, where all lines are essentially on-shell.

6. Diagrams for $\pi q \to \gamma^* q$, $\gamma^* \to \mu^+\mu^-$. Solid single lines represent quarks. Symbols p_1, p_a, p_b and p_c denote four-momenta of quarks, and k is the four-momentum of the gluon.

7. Polarization parameter α as a function of x_a for $\pi^- N \to \mu\bar{\mu}X$ at 225 GeV/c; α is obtained from fits to the data with the form $d\sigma/d\cos\theta \propto (1 + \alpha\cos^2\theta)$. The curve is a prediction of the model discussed in the text. Data are from Ref.4.

Blank Page

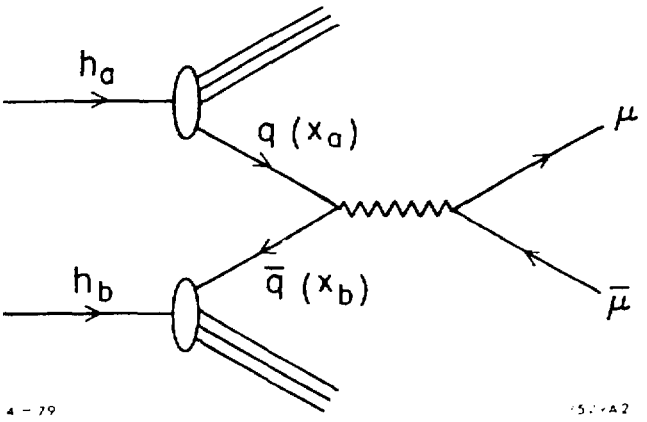

Fig. 1

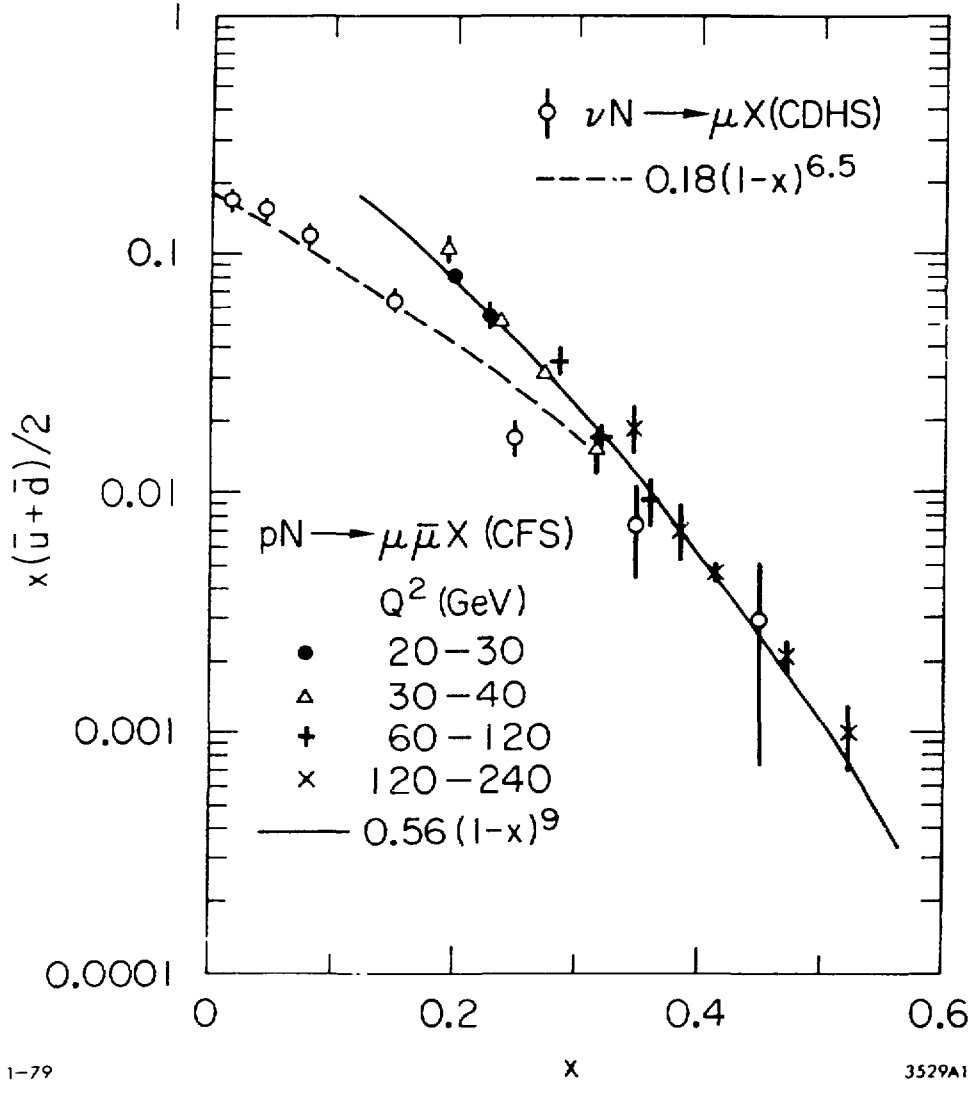
1
0.1
0.01
0.001
0.0001
0
0.2
0.4
0.6
x
$x(\bar{u}+\bar{d})/2$
$\nu N \rightarrow \mu X$(CDHS)
$0.18(1-x)^{6.5}$
$pN \rightarrow \mu\bar{\mu}X$ (CFS)
Q^2 (GeV)
20–30
30–40
60–120
120–240
$0.56(1-x)^9$
1–79
3529A1

Fig. 2

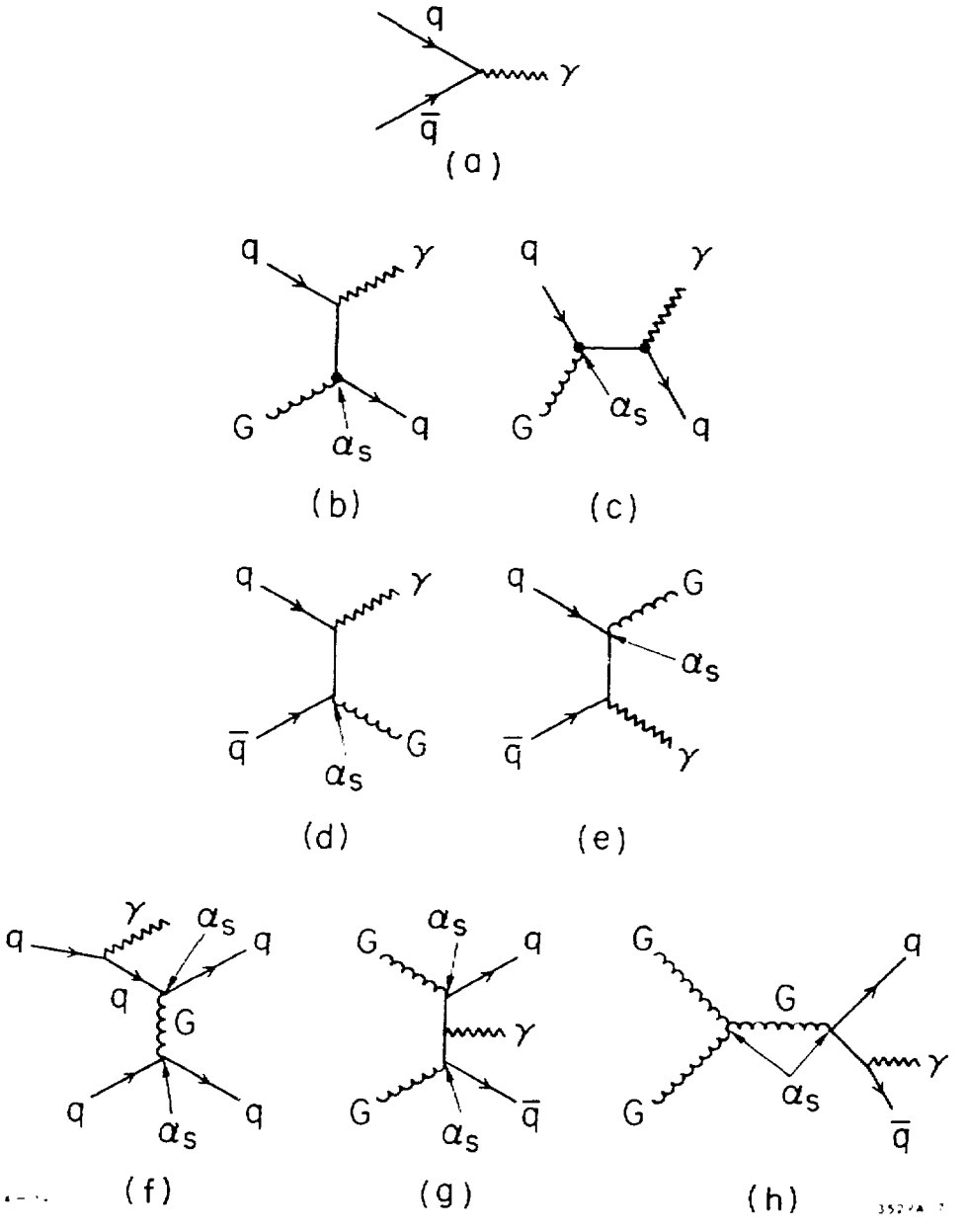
q
γ
q̄
(a)
q
γ
G
αs
q
(b)
q
γ
G
αs
q
(c)
q
γ
q̄
G
αs
(d)
q
G
αs
q̄
γ
(e)
γ
αs
q
q
G
q
q
αs
q
(f)
αs
G
q
γ
G
αs
q̄
(g)
G
q
G
γ
G
αs
q̄
(h)

Fig. 3

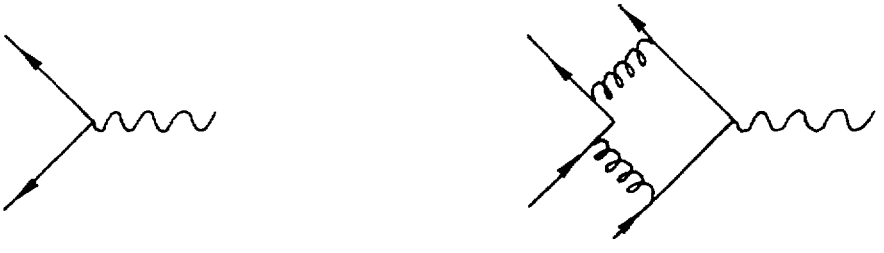

Fig. 4

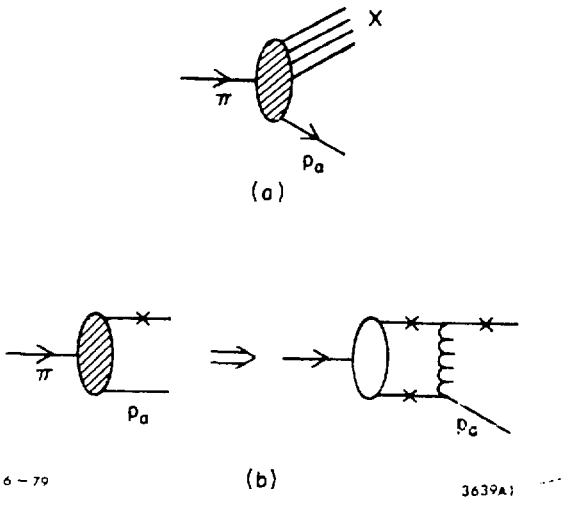

Fig. 5

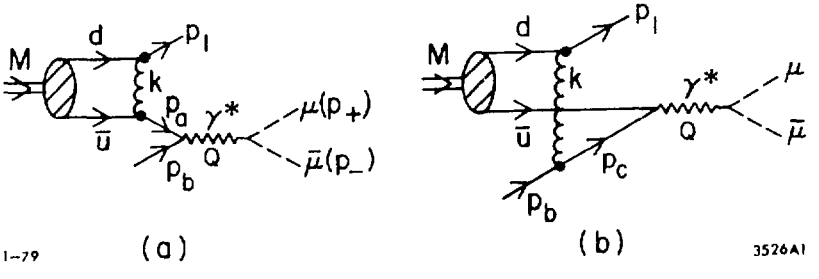
M
d
p_l
k
p_a
γ^*
$\mu(p_+)$
$\bar{u}$
$\bar{\mu}(p_-)$
p_b
Q
(a)
1-79
M
d
p_l
k
γ^*
μ
$\bar{u}$
Q
$\bar{\mu}$
p_c
p_b
(b)
3526A1

Fig. 6

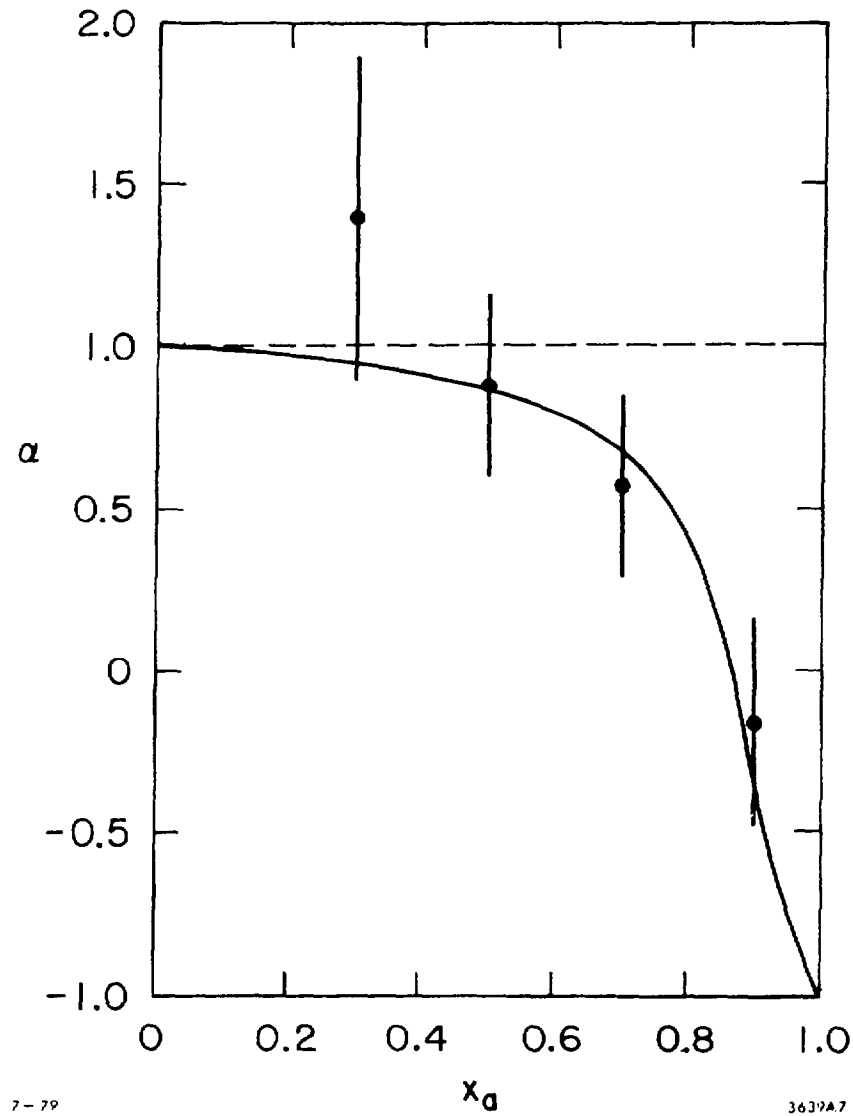

Fig. 7